Canadian Science Publishing
NRC Research Press journals | Publishing Services

Canadian Geotechnical Journal
Revue canadienne de géotechnique

Experimental Simulation and Mathematical Modelling of Clogging in Stone Column

Journal:	*Canadian Geotechnical Journal*
Manuscript ID	cgj-2017-0271.R1
Manuscript Type:	Article
Date Submitted by the Author:	01-Aug-2017
Complete List of Authors:	Tai, Pei; University of Wollongong Indraratna, Buddhima; University of Wollongong, Rujikiatkamjorn, Cholachat; University of Wollongong,
Keyword:	Clogging, stone column, consolidation model, model test, computed-tomography

Experimental Simulation and Mathematical Modelling of Clogging in Stone Column

Pei Tai

PhD candidate, MEng

Centre for Geomechanics and Railway Engineering,

School of Civil Engineering, Faculty of Engineering and Information Sciences,

University of Wollongong, Wollongong City, NSW 2522, Australia

Buddhima Indraratna

PhD (Alberta), MSc (Lond.), BSc (Hons., Lond.), DIC, FIEAust., FASCE, FGS

Distinguished Professor of Civil Engineering, Faculty of Engineering and Information Sciences,

Director, Centre for Geomechanics and Railway Engineering; University of Wollongong, Wollongong City, NSW 2522, Australia

Cholachat Rujikiatkamjorn

BEng (Hons), MEng (AIT), PhD (Wollongong)

Associate Professor of Civil Engineering, Centre for Geomechanics and Railway Engineering, Faculty of Engineering and Information Sciences, University of Wollongong, Wollongong City, NSW 2522, Australia

Author for correspondence:

Prof. B. Indraratna
Faculty of Engineering
University of Wollongong
Wollongong, NSW 2522, Australia.
Ph: +61 2 4221 3046
Fax: +61 2 4221 3238
Email: indra@uow.edu.au

Submitted to: Canadian Geotechnical Journal (cgj-2017-0271)

Experimental Simulation and Mathematical Modelling of Clogging in Stone Column

Abstract

In this paper, time-dependent clogging is studied considering a unit cell consisting of a single stone column interacting with the surrounding soft clay in this paper. Clogging is assessed quantitatively and the corresponding void space of the column is determined using computed-tomography (CT). It is observed that the extent of clogging is substantial in the upper part of the column, but diminishes rapidly with depth. The soil properties in the clogged zone are determined indirectly through additional tests of clay-aggregates mixtures with various clay fractions. An equal strain consolidation model based on the principle of unit cell analysis is developed to capture both the initial and time-dependent clogging. The model accounts for a reduction in permeability and an increase in compressibility of the column. This current model, as expected, offers identical results to some previous studies if clogging is ignored, while the comparison with other selected models demonstrates the influence that clogging of stone column can have on the consolidation of the surrounding soil. Furthermore, load-settlement predictions from the proposed 'equal strain' model are also compared to the consolidation response of a previously developed 'free strain' model.

Keywords: Clogging, stone column, consolidation model, model test, computed-tomography.

Introduction

Use of stone columns is a popular soft ground improvement technique that can readily shorten the drainage path and consolidation time, as well as increasing the stiffness and shear strength of the overall foundation. The short term stability of stone column has been studied in the field by Hughes et al. (1975) to validate their theory for estimating the ultimate load of isolated stone column. The long-term consolidation process of stone columns supported embankments has also been monitored to study the effectiveness of this method (Cooper and Rose 1999; Oh et al. 2007; Castro and Sagaseta 2009a). It has been stated that design of ground improved by stone columns requires to make sure there is "adequate bearing capacity" and "acceptable settlement performance" (Bouassida and Carter 2014). For the latter one, predicting the settlement of soft ground improved with stone column is generally inherited from the traditional radial consolidation theory as also applied to vertical drains. Balaam and Booker (1981) estimated the rate of settlement under granular piles by solving three dimensional consolidation equations (Biot 1941) numerically. Han and Ye (2001, 2002) computed the rate of consolidation of foundations reinforced with stone column with and without considering the effect of well resistance and soil disturbance(smear). Castro and Sagaseta (2009b) determined the extent of radial consolidation by including both the vertical and radial deformations of the stone column. Wang (2009) proposed a solution for soil consolidation effected by stone column under time-dependent loading. Xie et al. (2009) and Lu et al. (2010) proposed solutions which incorporated a coupled flow-deformation analysis, and these efforts revealed how the consolidation rate in some past studies (Han and Ye 2002; Zhang et al. 2006) were overestimated. Castro and Sagaseta (2011) compared various analytical solutions in tandem with the finite element analysis, and they implied that it was still reasonable to assume elastic soil behaviour for the surrounding

clay adjoining the stone column for certain cases, where the applied load would only lead to relatively small deformations.

Clogging of stone columns is derived from a mixture of column material and peripheral clay; it is a physical process rather than a biological or chemical cause. Physical clogging is a process whereby fine particles accumulate in the pore space of porous media by infiltration (Yong et al. 2013). Clogging related issues can generally be divided into two categories: the stability or erosion of base soil structures which provides fine base particles (Indraratna and Vafai 1997), and the serviceability of the drainage layer such as filters or pavements which are in contact with the base soil (Siriwardene et al. 2007). Clogging of stone columns should fall into the second category. Clogging induced by the installation of stone columns has also been confirmed by centrifuge tests (Weber et al. 2010). Indraratna et al. (2013) stated that the consolidation of the surrounding soil would be reduced by initial clogging of column based on a numerical simulation, and subsequently, Basack et al. (2015) extended this model to capture time-dependent clogging. Deb and Shiyamalaa (2015) also proposed to include time-dependent clogging by considering reduced permeability with time.

Even though past research studies highlighted the importance of incorporating clogging in the analysis of consolidation, to the best of the authors' knowledge, studies which quantified clogging accurately have rarely been reported. One of the key objectives of this paper is to provide a detailed model test where clogging of stone column is assessed quantitatively. To deliver it, a single model column and its surrounding clay was compressed one dimensionally (unit cell analysis), and after consolidation a core sample was extracted and scanned using the computed-tomography (CT) technique. Subsequently the extent of the clogging zone was evaluated and the porosity of the granular mass could be calculated. The load-settlement

response of this model test together with a past study (Basack et al. 2015) was then used to verify the newly proposed consolidation model. This consolidation model was solved numerically, and comparisons were then made with those solutions found in literature.

Categorisation of Clogging

The mechanisms of clogging in stone columns are different at various stages. Compaction or vibration is the main reason why clogging initiates during installation as the force applied to densify stone columns pushes the column material into the surrounding clay and thereby squeezes the fine soil grains into the gravel voids. This means clogging already exists in the column to start with before consolidation begins. However, clogging can also develop during soil consolidation where the clay particles are forced to move laterally, and then become trapped at pore constrictions and continue to accumulate with time. Although the pores in stone column are larger than the clay particles, clogging can still occur due to bridges formed at the pore constrictions (Valdes and Santamarina 2006) or initiating self-filtration (Reddi et al. 2000).

During installation, some initial clogging is inevitable, as the clay and granular material mix over a short period, compared to the time needed for soil consolidation. The properties of a clogged column depend on the amount of clay that intrudes into the column skeleton. Permeability will decrease in this area of the column if the clay particles reduce the void ratio and obstruct the moisture movement. However, the compressibility of the clogged zone will increase if the retained clay is sufficient to reduce the inter-particle contact (friction). Previous studies state that time-dependent clogging is influenced by the diameter ratio of large particles to fine particles, the porosity of coarse material, the flow rate, fluid viscosity, suspended particle concentration etc. (Huston and Fox 2015; Reddi et al. 2000; Valdes and Santamarina 2006). A reduction in

permeability due to clogging is generally understood based on the Kozeny-Carman theory which is widely used to predict the hydro-mechanical behaviour of a porous medium (Carrier III 2003). Albeit variations of this original mathematical formulations, the intrinsic relationship that makes permeability to diminish as the porosity of the medium decreases is always valid (DeLeo 1995). While the amount of retained base soil particles increases over time, the accumulated mass of trapped soil tends to decrease with distance from the inflow boundary (Alem et al. 2015). For the case of clogging in stone column, these findings mean that the extent of clogging would develop over time while the maximum reduction in permeability of the column is expected at the close proximity to the soil/column boundary.

Model Test and Clogging Identification

The material for the model column was prepared from crushed basalt taken from a quarry near Wollongong (NSW, Australia). Commercial kaolin clay was selected as base soil for the model test. The properties of these materials are summarised in Table 1, and the gradations of column material and kaolin clay are given in Figure 1(a). The kaolin clay was prepared as a slurry with 67% water content (1.2 times liquid limit), and then placed into a 760mm long cylindrical sample (300mm in diameter) wrapped in a rubber membrane inside a 1-D loading rig (Figure 1(b)). A top load of 65kPa was gradually applied to induce pre-compression, after which the clay would achieve an undrained shear strength of about 15kPa, and the initially prepared clay specimen would then be around 600mm high (i.e. height/diameter ratio of 2). Subsequently, a stone column consisting of crushed basalt was installed using a procedure simulating the 'replacement method' in the field. This cylindrical column had a 50-55 mm radius at the top surface and weighed 7.75 kg, and had an average void ratio of the granular assembly to be about 0.96. The specimen was then placed under a vertical stress which was gradually increased from

65kPa to 210kPa. This top load was applied through a rigid and permeable steel piston to simulate the condition of "equal strain" (Barron 1948). During consolidation, only top drainage of the column was permitted, and the loading force and surface settlement were recorded continuously; this will be discussed later and compared to the theoretical predictions.

After consolidation, a small test specimen (250mm in diameter and 450mm high) as shown in Figure 1, was cored and retrieved using a sharpened PVC tube and then digitally imaged on a CT (Computed Tomography) scanner (Toshiba Asteion S4), which can be classified as of a high resolution type with a precision of 0.2mm. CT scanning technique is a high voltage non-destructive method, whereby when X-rays penetrate the target, the amount of attenuated X-rays shows its density difference. A longitudinal section was obtained to show the deformation of the entire column, and then 82 cross sectional scans at different depths were obtained to examine the transition area at the boundary of the column and surrounding clay. A typical cross-sectional CT image is shown in Figure 2(a). The central circular part which represents the clean column was cropped and binarized after adopting a grayscale threshold (Otsu 1975), as shown in Figure 2(b) and (c) respectively. Here the black pixels correspond to the pores and the white pixels the solid gravel particles. After binarization, the ratio of black pixels to all the pixels represents the porosity of the column. The mean value of porosity for all the images was slightly less than 0.5, which generally agreed with the void ratio of 0.96 that was determined earlier.

For a given volume of granular mass of this stone column, if the entire void space between coarse particles is fully occupied by infiltrated clay, then the clay fraction in the clogged medium can be determined in the range of 0.32-0.34, which is defined as the volume of fines in a unit volume of solids containing both fines and coarse grains (Simpson and Evans 2016). It is also stated by Simpson and Evans (2016) that when the clay fraction approaches a threshold of 0.2, it

"demarcates a transition from a state where all coarse particles are touching each other", i.e., clay would begin displacing the coarse particles of the granular medium and break their contact beyond this threshold. The clay fraction in the current model test is certainly beyond this threshold.

The boundary of the clogged zone along the depth was determined as shown in Figure 3(a), and it quantitatively shows that clogging decreases in severity with depth. In terms of radius, the clogged zone occupies up to 20% of the outer ring of the entire column at the top 50mm, while it then decreases to around 10% at a depth of 50-100mm, and is even less than 5% for the remainder. A possible explanation is as follows. Drainage is provided only at the top of the specimen, and the applied stress reaches a maximum at the top, and diminishes with depth. This makes the top of the soil specimen become more affected by the hydraulic gradients generated in the shallow section of the soil compared to the deeper zone. As a result, a greater degree of soil is expected to be eroded into the column near the surface.

Moreover, the model column retains its cylindrical shape well after consolidation without any notable bulging. Photo images of the top surface of column before and after the test are also shown in Figure 3(b) and (c) respectively. These images confirm that clogging is severe at the top column section while the internal part of the column remains relatively unaffected. Specimens were also extracted from the surrounding clay after testing to detect any soil disturbance. The void ratios at different radii and depths were between 0.96 and 1.14, and the corresponding horizontal permeability of the surrounding clay varied in the range of $1.4\text{-}1.9\times10^{-9}$ m/s based on the empirical approach proposed by Al-Tabbaa and Wood (1987). It seems likely that no significant disturbance to the surrounding clay has occurred during column installation.

Consolidation Model Considering Time-dependent Clogging

To capture the effect of clogging of column on the soil consolidation, a mathematical description was deemed necessary. Besides the dependence on time, the property of a clogged column also alters with the radius and depth, so for simplicity, the average properties of different zones of the column are used. As shown in Figure 4(a), this schematic illustration of the model column consists of a clean section and a clogged zone, and the clay area is divided into disturbed and undisturbed zones. The clogged zone is subdivided into two portions which correspond to initial clogging during installation and time-dependent clogging during consolidation, respectively. The average soil properties are assigned to each zone, and the extent of clogging is then simulated by moving the boundary between the clean section of the column and the clogged zone, as shown in Figure 4(b).

The principle exploited to obtain the mean permeability of the whole column is such that the water flow out of the column at a given time is assumed to remain constant at any depth. The mean compressibility is then determined by assuming that the vertical strain is the same for the clogged zone and the clean column (i.e. equal strain). The average permeability and compressibility can then be computed as:

$$\bar{k}_c(t) = \frac{k_c r_{cl}^2(t) + k_{cl}(r_c^2 - r_{cl}^2(t))}{r_c^2} \tag{1a}$$

$$\bar{m}_{vc}(t) = \frac{r_c^2}{\frac{r_{cl}^2(t)}{m_{vc}} + \frac{r_c^2 - r_{cl}^2(t)}{m_{vcl}}} \tag{1b}$$

where $\bar{k}_c(t)$ and $\bar{m}_{vc}(t)$ are functions of time which are used to define column permeability and compressibility respectively, k_c and k_{cl} are the permeability of soil in the clean column and in the clogged zone respectively, m_{vc} and m_{vcl} are the coefficients of volume compressibility of soil in

the clean column and clogged zone respectively, $r_{cl}(t)$ is a mathematical function to define the time-dependent boundary between the clean column and clogged zone, , and r_c is the radius of the column.

Two modes of clogging are hypothesized here; the first mode, as noted by "I" in Figure 5, shows that the clogging area extends linearly with time until a critical time, whereas in type "II" the radius of the clean column decreases exponentially until it is stable. The progress of clogging can then be described mathematically as follows:

$$\text{I:}\quad r_{cl}(t) = \begin{cases} r_{ci} - t\frac{r_{ci}-r_{cl}}{t_c} & (0 \le t < t_c) \\ r_{cl} & (t \ge t_c) \end{cases} \tag{2a}$$

$$\text{II:}\quad r_{cl}(t) = r_{cl} + (r_{ci} - r_{cl})e^{-4.6t/t_c} \tag{2b}$$

where r_{ci} represents the boundary of the clean column and the clogged zone after initial clogging, and r_{cl} is the final radius of the clean section of the column; t_c is the time when clogging is complete for pattern I, and when the time-dependent clogging area expands to 99% of its final value for pattern II. For pattern II, due to the exponential function used, 100% can only be reached when time approaches infinity, so the constant, -4.6, in Eqn. (2b) corresponds to 99% when the time reaches a critical value, t_c.

Governing equations

Several basic assumptions are declared herein:

i. Due to the adoption of equal strain hypothesis for this unit cell, only the vertical strain is considered and it is assumed to be uniform regardless of the radius at any depth;

ii. Traditional linear Darcy's law is assumed to be valid;

iii. Only vertical flow is considered in column, while only radial flow is considered in the surrounding clay. Pore pressure in the clay varies with the radius and depth;

iv. The load on top of the unit cell is applied instantaneously and then held constant.

Considering the unit cell (Fig. 4), the stress distributions can then be determined through the effective stress principle as,

$$\pi(r_s^2 - r_c^2)\bar{\sigma}_s + \pi r_c^2 \bar{\sigma}_c = \pi r_s^2 \sigma \quad (3)$$

$$\bar{m}_{vs}(\bar{\sigma}_s - \bar{u}_s) = \bar{m}_{vc}(t)(\bar{\sigma}_c - u_c) = \varepsilon_v \quad (4)$$

$$\bar{m}_{vs} = \frac{r_s^2 - r_c^2}{\int_{r_c}^{r_s} \frac{2\pi r}{m_{vs}(r)} dr} \quad (5)$$

where $\bar{\sigma}_s$ and $\bar{\sigma}_c$ are the average total vertical stresses on the surrounding soil and the column at any depth respectively; $\bar{u}_s$ is the average excess pore pressure in the surrounding soil at any depth; u_c is the excess pore pressure in the column at any depth; $\bar{m}_{vs}$ is the average coefficient of volume compressibility of the surrounding soil; $m_{vs}(r)$ is a function of the radius for defining the variation of coefficient of volume compressibility in the surrounding soil; r_s is the radius of the influence zone, and ε_v is the vertical strain of both the column and the surrounding soil.

The compressibility of column varies with time due to clogging; not only it would affect the vertical strain directly according to Eqn. (4), but also the changing stiffness ratio of column to clay would influence the build-up of excess pore water pressure. In this way, the 'equal strain' analysis is expected to give different pore pressure and consolidation results compared to the previous 'free strain' analysis of a unit cell (e.g. Indraratna et al. 2013; Basack et al. 2015).

For equal strain condition, the average excess pore water pressure at a given depth of the unit cell $\bar{u}$ and the corresponding rate of vertical strain at the same depth can be expressed by:

$$\bar{u} = \frac{1}{\pi r_s^2}\left(\bar{u}_s \int_{r_c}^{r_s} 2\pi r dr + u_c \int_0^{r_c} 2\pi r dr\right) \quad (6a)$$

$$\frac{\partial \varepsilon_v}{\partial t} = \frac{\partial[\bar{m}_v(t) \cdot (\sigma - \bar{u})]}{\partial t} \quad (6b)$$

$$\bar{m}_v(t) = \frac{r_s^2}{\frac{r_c^2}{\bar{m}_{vc}(t)} + \frac{r_s^2 - r_c^2}{\bar{m}_{vs}}} \quad (6c)$$

where $\bar{m}_v(t)$ is the coefficient of volume compressibility of the unit cell.

If the column compressibility is made equal to that of the surrounding clay, then the current problem will become the same as radial consolidation of a vertical drain system. On the contrary, if the compressibility ratio of column to clay is made to decrease to a sufficient low value, then the vertical strain of the unit cell will diminish considerably to an extent that the soil consolidation will become negligible; thereby approaching a single pile foundation system.

If the volume change of the surrounding soil equals the change in flow volume, the following equation can describe the consolidation of surrounding clay:

$$\frac{1}{\gamma_w r}\frac{\partial}{\partial r}\left(k_s \cdot f(r) \cdot r \cdot \frac{\partial u_s}{\partial r}\right) = -\frac{\partial \varepsilon_v}{\partial t} \quad (7)$$

where k_s is the permeability of undisturbed clay, f(r) is a function used to describe the varying permeability of surrounding clay with radius, γ_w is the unit weight of water, and u_s is the excess pore pressure at a certain point in the surrounding clay.

The governing equation for the column can then be derived by assuming the column deformation to be equal to the net water flow, thus,

$$\frac{2k_s}{\gamma_w r_c}\frac{\partial u_s}{\partial r}\bigg|_{r=r_c} + \frac{\bar{k}_c(t)}{\gamma_w}\frac{\partial^2 u_c}{\partial z^2} = -\frac{\partial \varepsilon_v}{\partial t} \quad (8)$$

Based on the unit cell hypothesis and strain compatibility requirement, the following boundary conditions are applied:

i. No water flow at the cylindrical surface and the bottom of unit cell;

ii. The pore pressure is continuous at the column-clay interface;

iii. Zero excess pore water pressure at the top surface (free-draining);

iv. The initial pore water pressure is assumed to be the same as the initial loading intensity.

Given the unit cell height as "h", these boundary conditions can be expressed mathematically as:

$$\left.\frac{\partial u_s}{\partial r}\right|_{r=r_s} = 0 \tag{9a}$$

$$\frac{\partial \bar{u}_s(h,t)}{\partial z} = \frac{\partial u_c(h,t)}{\partial z} = 0 \tag{9b}$$

$$u_s = u_c(r = r_c) \tag{9c}$$

$$\bar{u}_s(0,t) = u_c(0,t) = 0 \tag{9d}$$

$$\bar{u}_s(z,0) = u_c(z,0) = \sigma \ \ (z > 0) \tag{9e}$$

To combine the consolidation of column and surrounding clay, several mathematical manipulations are made to obtain a unified governing equation (see Appendix for derivation).

$$\bar{m}_v(t)\frac{\partial^3 \bar{u}}{\partial z^2 \partial t} + [\bar{m}_v{}'(t) + B]\frac{\partial^2 \bar{u}}{\partial z^2} + C\frac{\bar{m}_v(t)}{\bar{k}_c(t)}\frac{\partial \bar{u}}{\partial t} + C\frac{\bar{m}_v{}'(t)}{\bar{k}_c(t)}\bar{u} = C\sigma\frac{\bar{m}_v{}'(t)}{\bar{k}_c(t)} \tag{10a}$$

$$A = \int_{r_c}^{r_s} r \int_{r_c}^{r} \frac{r_s^2 - r^2}{f(r)r}\, dr\, dr \tag{10b}$$

$$B = \frac{k_s r_s^2}{A\gamma_w} \tag{10c}$$

$$C = -\frac{k_s r_s^4}{A r_c^2} \tag{10d}$$

A collation of the mathematical consolidation models for soil improved by stone columns is enumerated in Table 2, in comparison with the current model.

Mathematical solution for 'no clogging' and 'clogging'

Eqn. (10) is a high-order non-homogeneous linear partial differential equation, so no existing method can be used directly to solve it. However, as suggested by various studies (Lei et al. 2015; Leo 2004; Lu et al. 2010; Tang and Onitsuka 1998), the mean excess pore water pressure at a given depth of unit cell can be expressed using a Fourier series expansion, such as

$$\bar{u} = \sum_{n=1}^{\infty} T_n(t) \cdot sin(\alpha_n z) \tag{11a}$$

$$\alpha_n = \frac{2n-1}{2h}\pi \tag{11b}$$

The item on the right-hand side of Eqn. (10a) can also be expanded to a sinusoidal series, hence,

$$C\sigma \frac{\bar{m}_v{}'(t)}{\bar{k}_c(t)} = \frac{2C\sigma}{\alpha_n h}\frac{\bar{m}_v{}'(t)}{\bar{k}_c(t)} \sum_{n=1}^{\infty} sin(\alpha_n z) \tag{12}$$

Substituting Eqns. (11a) and (12) into Eqn. (10a), the following non-homogeneous ordinary differential equation is obtained,

$$T_n{}'(t)\bar{m}_v(t)\left(\frac{C}{\bar{k}_c(t)} - \alpha_n^2\right) + T_n(t)[C\frac{\bar{m}_v{}'(t)}{\bar{k}_c(t)} - \alpha_n^2(\bar{m}_v{}'(t) + B)] = \frac{2C\sigma}{\alpha_n h}\frac{\bar{m}_v{}'(t)}{\bar{k}_c(t)} \tag{13}$$

The solution to Eqn. (13) cannot be derived by explicit integrals, but the function $T_n(t)$ could be solved numerically using the Runge-Kutta method. The average degree of consolidation in terms of excess pore water pressure for the unit cell $\bar{U}$, which changes with dimensionless time factor T, is then given by the following:

$$\bar{U} = 1 - \frac{\int_0^h \bar{u} dz}{\sigma h} = 1 - \sum_{n=1}^{\infty} \frac{T_n(T)}{\sigma h \alpha_n} \tag{14a}$$

$$T = \frac{k_s}{4 m_{vs} \gamma_w r_s^2} t \tag{14b}$$

Case of 'no clogging'

In the absence of clogging, Eqn. (10a) simplifies to the form below,

$$\bar{m}_v \left(\frac{C}{k_c} - \alpha_n^2 \right) T_n'(t) - B \alpha_n^2 T_n(t) = 0 \tag{15a}$$

$$\bar{m}_v = \frac{r_s^2}{\frac{r_c^2}{m_{vc}} + \frac{r_s^2 - r_c^2}{\bar{m}_{vs}}} \tag{15b}$$

An analytical solution for the average pore water pressure and the corresponding degree of consolidation can now be readily obtained for the case of no clogging, thus:

$$\bar{u} = \sum_{n=1}^{\infty} \frac{2\sigma}{\alpha_n h} \cdot e^{\frac{-B \alpha_n^2 k_c t}{\bar{m}_v (\alpha_n^2 k_c - C)}} \cdot sin(\alpha_n z) \tag{16a}$$

$$\bar{U} = 1 - \sum_{n=1}^{\infty} \frac{2}{\alpha_n^2 h^2} e^{\frac{-B \alpha_n^2 k_c t}{\bar{m}_v (\alpha_n^2 k_c - C)}} \tag{16b}$$

The case of 'no clogging' is now considered with parameters obtained from Indraratna et al. (2013), although the permeability of column is chosen according to Han and Ye (2002). The parameters for this case of 'no clogging' are listed in Table 3.

The consolidation curves of different models are computed and plotted in Figure 6. The estimation of the average degree of consolidation given by the current model is almost identical to the previous solutions of 'equal strain' models (Han and Ye 2002; Lu et al. 2010). The

prediction by model of Indraratna et al. (2013) underestimates consolidation, possibly because of its 'free strain' hypothesis.

Case of clogging

The effect of clogging has also been studied using the same case above but with additional clogging related parameters incorporated in the analysis. Indraratna et al. (2013) introduced two parameters to describe and support the concept of initial clogging: (i) the ratio of clogged radius to the size of column, α; (ii) the ratio of clogged permeability to clean column permeability, α_k. In contrast, time-dependent clogging has been described based on release coefficient α_0 and capture coefficient β (Deb and Shiyamalaa 2015). The clogged zone was evaluated to be as much as 20% in the current study, while the "penetration zone" was reported elsewhere to be about 30% (Weber et al. 2010). Based on these findings, a more conservative condition is assumed where a clogging zone over time is assumed to occupy the outer 30% of the column radius, and any initial clogging is ignored. The clogging related parameters are also given in Table 3.

The current model prediction in comparison with above mentioned two models (i.e. initial clogging and time-dependent clogging) is plotted in Figure 7. The results show that the model proposed by Deb and Shiyamalaa (2015) predicts a faster consolidation rate, while the model by Indraratna et al. (2013) gives a lower degree of consolidation ($\bar{U}$) for the same time factor (T). The effect of omitting the change of column compressibility by Deb and Shiyamalaa (2015) could be the reason of a faster consolidation prediction. Moreover, in the model proposed by Indraratna et al. (2013), the 'worst-case scenario' was considered where maximum clogging would occur at the initial stage, therefore, the subsequent consolidation rate is significantly impeded as expected.

Using the current model, different scenarios of clogging could be considered and simulated: (i) no time-dependent clogging ($r_{ci} = r_{cl}$), i.e. clogging is assumed to have finished initially before any consolidation; and (ii) linear and exponential patterns of clogging over time in lieu of initial clogging ($r_{ci} = r_c$). Through comparison of these scenarios, it is also observed (Fig. 7) that the assumption of maximum clogging at the initial stage can delay the consolidation process further compared to the time-dependent clogging models, and that there will be further delay in consolidation if the clogging process follows pattern II (exponential) instead of pattern I (linear).

Theoretical Model Validation by Physical Modelling

In this final section of the paper, the proposed consolidation model formulated and described earlier will be validated using two laboratory physical model tests. One of them was elaborated given earlier in the 'Model Test' section. The other one was reported by Basack et al. (2015).

The soil properties in the clogged zone are difficult to measure directly due to its small dimension. Therefore attempt was made to reproduce the soil mixture and examine how the properties of the mixture change with varying clay fractions. In this regard, different clay fractions were used to make several cylindrical samples and pre-loaded before conducting falling head permeability tests and compression tests to determine the relevant permeability and compressibility properties. These properties were then compared to previous data (Simpson and Evans 2016; Watabe et al. 2011) as shown in Figure 8. The current test results agree well with previous data. Due to different size of coarse particles and loading paths used in various tests, two normalized parameters are defined to compare the results, hence,

$$\Delta m_v = \frac{m_{vm} - m_{vc}}{m_{vf} - m_{vc}} \qquad (17a)$$

$$\Delta k = \frac{\lg(k_c) - \lg(k_m)}{\lg(k_c) - \lg(k_f)} \quad (17b)$$

where Δk and Δm_v are the normalized permeability and compressibility variation respectively; k_c and m_{vc} are the permeability and compressibility of coarse aggregates respectively; k_f and m_{vf} are the permeability and compressibility of the fines respectively; k_m and m_{vm} are the permeability and compressibility of the mixture, respectively.

The parameters used to predict model tests are listed in Table 4. The properties of the clean column and surrounding clay were obtained in the laboratory as discussed earlier. Because of the smaller particle size, the stiffness of model column was lower than the value of 48-120 MPa as mentioned in previous studies (Ambily and Gandhi 2007; Arulrajah et al. 2009; Fatahi et al. 2012). There was no disturbance to pure clay outside the column as indicated by the measurement of void ratio of the surrounding clay after testing. The soil properties in the clogged zone were selected based on best-fit regression for a determined clay fraction of 0.32 (Fig. 8).

A comparison between the current model test and corresponding theoretical predictions using Eqn. 6(b) is shown in Figure 9. If clogging is neglected, the settlement prediction is accurate only at the beginning, i.e. after the first stage of loading there is notable discrepancy, and the overall settlement is underestimated by about 15%. If clogging occurs initially, the calculated settlement is higher than the observed data during the first stage of loading, but then converges to the actual settlement curve. The calculations corresponding to the cases of 'no clogging' and 'initial clogging' provide upper and lower limits, respectively. Time-dependent clogging is more apparent according to the examination of photo images of the column surface before and after testing. Unfortunately clogging process (rate and extent) could not be quantified to define a critical time t_c accurately at which the soil consolidation is significantly influenced by the

clogging of the column. Both the reduction in permeability and the increase in compressibility were assumed to follow an exponential pattern (pattern II). It is observed that the calculated settlements agree with the laboratory measurements, if time-dependent clogging is considered with the appropriate choice of a value of t_c.

Figure 10 shows the comparisons using the current model based on time dependent clogging with the model proposed by Basack et al. (2015) together with the measured data. It is noted that the initial part of the load-settlement response of the test was not suitable for the application of current consolidation model due to the effect of unloading and recompression. Therefore, only the data after recompression was selected to verify the proposed model. The radius ratio of clean column to the whole column was reported to be 0.92 which is slightly lower than the current model test, but the relevant soil properties are not found, so they were chosen as the same value as the current model test. The results demonstrate that improved predictions can be made using the current unit cell model where clogging of the column can increase the overall compressibility of the unit cell under equal strain condition.

It is interesting to see that the corresponding settlement prediction with time-dependent clogging becomes higher than the case of 'no clogging'. The reasons for this can be explained as follows: clay intrusion in to the granular assembly can increase the column compressibility (i.e. reduction of inter-particle friction) hence the settlement at a given applied load in relation to the equal strain condition. Moreover, the stress distribution on top of the unit cell also varies (less load taken by the column) which could then lead to a greater stress transfer to the surrounding soil, hence an increased consolidation settlement of the clay. If the applied load is independent of time, the settlement would depend on both the degree of soil consolidation and the compressibility of the unit cell. The extent of clogging can actually increase the compressibility of the whole unit

cell thus the associated settlement. Slight clogging of stone column barely retards the rate of surrounding soil consolidation, while substantially increased clogging can impede drainage through the granular pile, requiring a greater time to attain the ultimate settlement. In this respect, it is perceived that a critical situation may exist below which the settlement can be adversely affected due to clogging. However, such an analysis that requires coupling of clay infiltration to the column with the soil consolidation theory is beyond the scope of this paper, and will be discussed in the future.

Conclusion

A detailed physical model test of a unit cell (i.e. single stone column) was conducted to study clogging, together with loading and settlement data. After consolidation, a core part of the model test sample was exhumed and an image analysis using computed tomography (CT scan) was employed to quantify the extent of clogging. It could be seen that the clogged zone progressed with consolidation and occupied almost 20% of the outer ring of the model column towards the top; the extent of clogging decreased rapidly with depth until it eventually vanished. The porosity of the column was also obtained through weight-volume calculations and from image analysis; the results from both methods showed a good agreement. These clogging parameters were then used to predict the consolidation behaviour, and compare with the laboratory measurements.

A consolidation model capturing both initial clogging and time-dependent clogging in a stone column unit cell was proposed, where the changes of properties of the stone column due to clogging were considered by different clogging patterns. The proposed model predictions were also compared with those of previous studies (with and without clogging); it is found that notable

discrepancies exist between models which involve clogging. The results under 'no clogging' and 'initial clogging' situations represented the upper and lower boundaries of the predictions. In particular, the current model with equal strain condition indicated that the clogging of column can lead to increased compression, because the intrusion of fines to the granular assembly at the column top can increase its compressibility, and thereby the overall settlement of the unit cell under the equal strain condition. This observation may be in conflict with the 'free strain' condition, where the clogging of the column and the corresponding reduction in excess pore pressure dissipation can lead to a decreased rate of soil consolidation.

Acknowledgements

The Authors thankfully acknowledge the financial support received from the Australian Research Council (ARC) and industry partners, namely Coffey Geotechnics and Keller Ground Engineering, in the form of an industry linkage project. The authors thank Dr. Ana Heitor for her help in conducting and processing CT scanning. The authors also thank Dr. Sudip Basack and Mr. Firman Siahaan for their constructive comments and discussions during the preparation of this paper. The authors are also grateful for the assistance provided by Mr. Ritchie McLean during the laboratory experiments.

References

Al-Tabbaa, A., and Wood, D.M. 1987. Some measurements of the permeability of kaolin. Géotechnique, 37(4): 499-514.

Alem, A., Ahfir, N.D., Elkawafi, A., and Wang, H.Q. 2015. Hydraulic operating conditions and particle concentration effects on physical clogging of a porous medium. Transport in Porous Media, 106(2): 303-321.

Ambily, A.P., and Gandhi, S.R. 2007. Behavior of stone columns based on experimental and FEM Analysis. Journal of Geotechnical and Geoenvironmental Engineering, 133(4): 405-415.

Arulrajah, A., Abdullah, A., Bo, M., and Bouazza, A. 2009. Ground improvement techniques for railway embankments. Proceedings of the Institution of Civil Engineers-Ground Improvement, 162(1): 3-14.

Balaam, N.P., and Booker, J.R. 1981. Analysis of Rigid Rafts supported by Granular Piles. International Journal for Numerical and Analytical Methods in Geomechanics, 5(4): 379-403.

Barron, R.A. 1948. The influence of drain wells on the consolidation of fine-grained soils. Diss., Providence, US Eng. Office.

Basack, S., Siahaan, F., Indraratna, B., and Rujikiatkamjorn, C. 2015. Influence of clogging on the performance of stone column improved soft ground, 15 th PanAmerican Conference on Soil Mechanics and Goetechnical Engineering.

Biot, M.A. 1941. General theory of three-dimensional consolidation. Journal of Applied Physics, 12(2): 155-164.

Bouassida, M., and Carter, J.P. 2014. Optimization of design of column-reinforced foundations. International Journal of Geomechanics: 04014031.

Carrier III, W.D. 2003. Goodbye, hazen; hello, kozeny-carman. Journal of Geotechnical and Geoenvironmental engineering, 129(11): 1054-1056.

Castro, J., and Sagaseta, C. 2009a. Field instrumentation of an embankment on stone columns, Proceedings of the 17th International Conference on Soil Mechanics and Geotechnical Engineering, Alexandria, Egypt, pp. 1865-1868.

Castro, J., and Sagaseta, C. 2009b. Consolidation around stone columns: influence of column deformation. International Journal for Numerical and Analytical Methods in Geomechanics, 33(7): 851-877.

Castro, J., and Sagaseta, C. 2011. Consolidation and deformation around stone columns: numerical evaluation of analytical solutions. Computers and Geotechnics, 38(3): 354-362.

Cooper, M., and Rose, A. 1999. Stone column support for an embankment on deep alluvial soils. Proceedings of the ICE-Geotechnical Engineering, 137(1): 15-25.

Deb, K., and Shiyamalaa, S. 2015. Effect of clogging on rate of consolidation of stone column-improved ground by considering particle migration. International Journal of Geomechanics: 04015017.

DeLeo, P. 1995. Microbial clogging of saturated soils and aquifer materials: Evaluation of mathematical models. Water Resources Research, 31(9): 2173-2180.

Fatahi, B., Basack, S., Premananda, S., and Khabbaz, H., 2012. Settlement prediction and back analysis of Young's modulus and dilation angle of stone columns. Australian Journal of Civil Engineering, 10(1): 67-79.

Han, J. and Ye, S.L. 2001. Simplified method for consolidation rate of stone column reinforced foundations. Journal of Geotechnical and Geoenvironmental Engineering, 127(7): 597-603.

Han, J. and Ye, S.L. 2002. A theoretical solution for consolidation rates of stone column-reinforced foundations accounting for smear and well resistance effects. The International Journal Geomechanics, 2(2): 135-151.

Hughes, J.M.O., Withers, N.J., and Greenwood, D.A. 1975. A field trial of the reinforcing effect of a stone column in soil. Géotechnique, 25(1): 31-44.

Huston, D.L. and Fox, J.F. 2015. Clogging of fine sediment within gravel substrates: dimensional analysis and macroanalysis of experiments in hydraulic flumes. Journal of Hydraulic Engineering, 141(8): 04015015.

Indraratna, B., Basack, S., and Rujikiatkamjorn, C. 2013. Numerical solution of stone column-improved soft soil considering arching, clogging, and smear Effects. Journal of Geotechnical and Geoenvironmental Engineering, 139(3): 377-394.

Indraratna, B., Ionescu, D., and Christie, H. 1998. Shear behavior of railway ballast based on large-scale triaxial tests. Journal of geotechnical and geoenvironmental Engineering, 124(5): 439-449.

Indraratna, B., and Vafai, F. 1997. Analytical model for particle migration within base soil-filter system. Journal of Geotechnical and Geoenvironmental Engineering, 123(2): 100-109.

Lei, G.H., Zheng, Q., Ng, C.W.W., Chiu, A.C.F., and Xu, B. 2015. An analytical solution for consolidation with vertical drains under multi-ramp loading. Géotechnique, 65(7): 531-547.

Leo, C.J. 2004. Equal strain consolidation by vertical drains. Journal of Geotechnical and Geoenvironmental engineering, 130(3): 316-327.

Lu, M.M., Xie, K.H., and Guo, B. 2010. Consolidation theory for a composite foundation considering radial and vertical flows within the column and the variation of soil permeability within the disturbed soil zone. Canadian Geotechnical Journal, 47(2): 207-217.

Ni, J., 2012. Application of geosynthetic vertical drains under cyclic loads in stabilizing tracks. Doctor of Philosophy, University of Wollongong, Wollongong.

Oh, E.Y.N., Balasubramaniam, A.S., Surarak, C., Bolton, M., Chai. G.W.K., Huang, M., and Braund, M. 2007. Behaviour of a highway embankment on stone column improved estuarine clay. Proc., 16th Southeast Asian Geotechnical Conf., Vol. 1, Southeast Asian Geotechnical Society, Bangkok, Thailand, 567–572.

Otsu, N. 1975. A threshold selection method from gray-level histograms. Automatica, 11(285-296): 23-27.

Reddi, L.N., Ming, X., Hajra, M.G., and Lee, I.M. 2000. Permeability reduction of soil filters due to physical clogging. Journal of Geotechnical and Geoenvironmental engineering, 126(3): 236-246.

Simpson, D.C., and Evans, T.M. 2016. Behavioral thresholds in mixtures of sand and kaolinite clay. Journal of Geotechnical and Geoenvironmental Engineering, 142(2): 04015073.

Siriwardene, N., Deletic, A., and Fletcher, T. 2007. Clogging of stormwater gravel infiltration systems and filters: Insights from a laboratory study. Water research, 41(7): 1433-1440.

Tang, X.W., and Onitsuka, K. 1998. Consolidation of ground with partially penetrated vertical drains. Geotechnical Engineering.

Valdes, J.R., and Santamarina, J.C. 2006. Particle clogging in radial flow: microscale mechanisms. SPE Journal, 11(02): 193-198.

Wang, G. 2009. Consolidation of soft clay foundations reinforced by stone columns under time-dependent loadings. Journal of Geotechnical and Geoenvironmental engineering, 135(12): 1922-1931.

Watabe, Y., Yamada, K., and Saitoh, K. 2011. Hydraulic conductivity and compressibility of mixtures of Nagoya clay with sand or bentonite. Géotechnique, 61(3): 211-219.

Weber, T.M., Peschke, G., Laue, J., PlöTze, M., and Springman, S.M. 2010. Smear zone identification and soil properties around stone columns constructed in-flight in centrifuge model tests. Géotechnique, 60(3): 197-206.

Xie, K.H., Lu, M.M., and Liu, G.B. 2009. Equal strain consolidation for stone columns reinforced foundation. International Journal for Numerical and Analytical Methods in Geomechanics, 33(15): 1721-1735.

Yong, C.F., McCarthy, D.T., and Deletic, A. 2013. Predicting physical clogging of porous and permeable pavements. Journal of Hydrology, 481: 48-55.

Zhang, Y., Xie, K.H., and Wang, Z. 2006. Consolidation analysis of composite ground improved by granular columns considering variation of permeability coefficient of soil. Geotechnical Special Publication, 152: 135.

List of Tables:

List of Figures:

Table 1. Properties of materials in model test

Properties of soil used in model test	
Kaolin Clay (commercial kaolin)	
Specific Gravity	[a]2.7
Liquid limit	[a]55
Plastic limit	[a]27
Compression Index	[a]0.42
Swelling Index	[a]0.06
Void ratio	[b]1.3/1.2
Vertical Permeability($\times 10^{-9}$m/s)	[c]1.3/1.1
Compression modulus (MPa)	[c]1/1.3
Aggregates (Crushed Basalt)	
LA abrasion value	[d]15%
Point load index (MPa)	[d]5.39
Specific Gravity	2.65
Void ratio	0.65-1.08
Permeability ($\times 10^{-5}$m/s)	1.9-4
Drained friction angle (Degrees)	47-52
Compression modulus (MPa)	[e]30-50

a. Obtained from Ni (2012)

b. Measured after 1D consolidation with 65kPa/110kPa vertical stress

c. Measured after anisotropic consolidation, σ_1'=65kPa/110kPa, σ_3'=50kPa

d. Value of Latite basalt from Indraratna et al. (1998)

e. Measured after isotropic consolidation, σ_3'=50kPa

Table 2. Comparison of consolidation models for stone column improved soil

Models	Clogging		Column deformation	Well resistance	Basic hypothesis
	Initial	Time dependent			
Han & Ye (2001, 2002)	N/A	N/A	N/A	Yes	Equal strain
Wang (2009)	N/A	N/A	N/A	Yes	Equal strain
Xie et al. (2009)	N/A	N/A	Yes	Yes	Equal strain
Lu et al. (2010)	N/A	N/A	Yes	Yes	Equal strain
Indraratna et al. (2013)	Yes	No	N/A	N/A	Free strain
Basack et al. (2015)	No	Yes	N/A	N/A	Free strain
Deb & Shiyamalaa (2015)	No	Yes	N/A	N/A	Equal strain
Current model	Yes	Yes	Yes	Yes	Equal strain

Table 3. Parameters for comparison of different consolidation models

Case of 'no clogging' (Indraratna et al. 2013)

k_c(m/s)	k_s(m/s)	k_d(m/s)	r_c(m)	r_s/r_c
[a] 1.6×10^{-6}	1.6×10^{-9}	1.6×10^{-10}	0.5	3
r_d/r_c	m_{vs}/m_{vc}	m_{vs}(MPa^{-1})	h(m)	
1.15	7	0.5	16	

Case of clogging

Indraratna et al. (2013)	$\alpha = 0.5$		$\alpha_k = 0.5$	
Deb & Shiyamalaa (2015)	$\alpha_0 = 4\times10^{-5}s^{-1}$		$\beta = 10^{-12}s^{-1}$	
Current model	m_{vcl}/m_{vc}	k_{cl}/k_c	r_{cl}/r_c	T_c (when $r_{ci} = r_c$)
	[b] 2	[b] 0.1	[b] 0.7	[b] 1

a. obtained from Han & Ye (2002)
b. assumed for the present analysis

Table 4. Parameters for predicting model tests

	Current model test	Model test by Basack et al. (2015)
k_c(m/s)	[a] 3×10^{-5}	–
k_s(m/s)	[a] 1.3×10^{-9}	10^{-9}
k_{cl}/k_c	[b] 10^{-3}	–
r_c(m)	[c] 0.055	0.05
r_s(m)	[c] 0.15	0.15
r_{cl}/r_c	0.9	0.92
h(m)	[c] 0.6	0.6
m_{vs}(MPa^{-1})	[a] 1	2
m_{vs}/m_{vc}	[a] 30	–
m_{vs}/m_{vcl}	[b] 3.9	–

a. chosen based on material tests
b. determined through fit line in Fig 8
c. measured directly

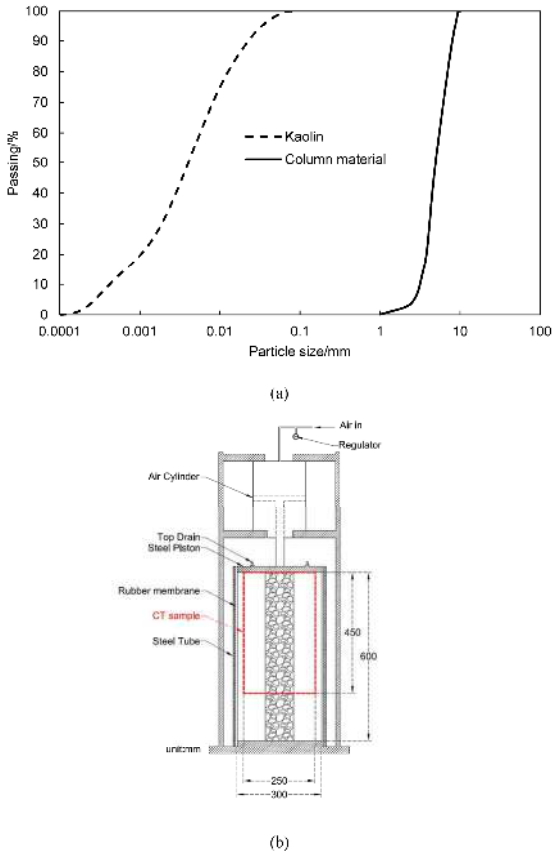

Fig. 1. (a) Gradations of material; (b) setup of model test

Fig 1. (a) Gradations of material; (b) setup of model test

297x420mm (300 x 300 DPI)

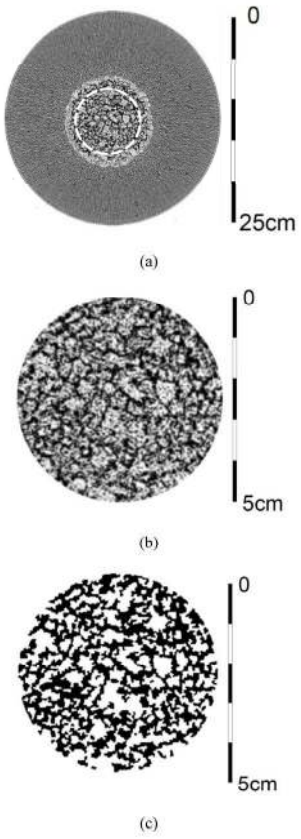

Fig 2. CT image of depth 15mm: (a) Original image; (b) clean column; (c) image of clean column after binarization

2

Fig 2. CT image of depth 15mm: (a) Original image; (b) clean column; (c) binarized image of clean column

297x420mm (300 x 300 DPI)

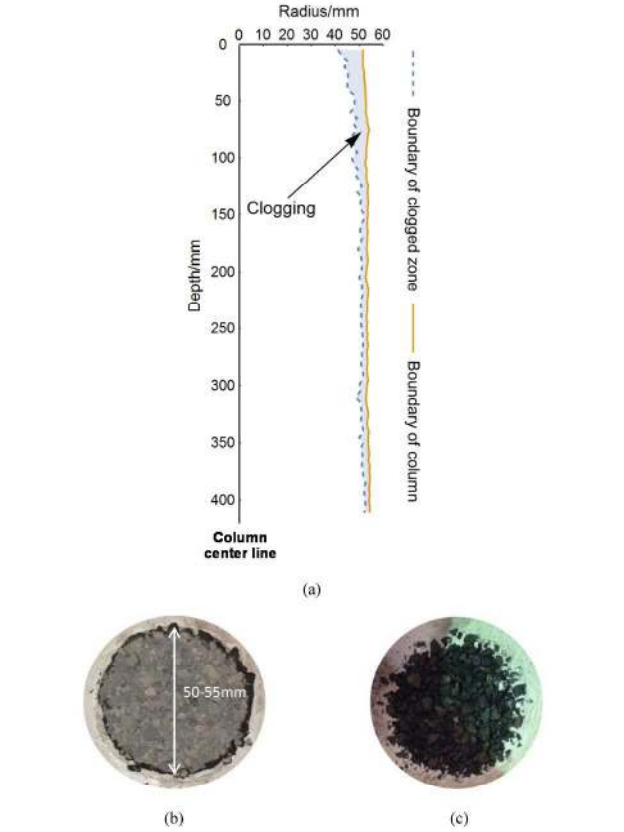

Fig 3. (a) Extent of clogging in the CT sample; (b) surface view before test; (c) surface view after test

Fig 3. (a) Extent of clogging in the CT sample; (b) surface view before test; (c) surface view after test

297x420mm (300 x 300 DPI)

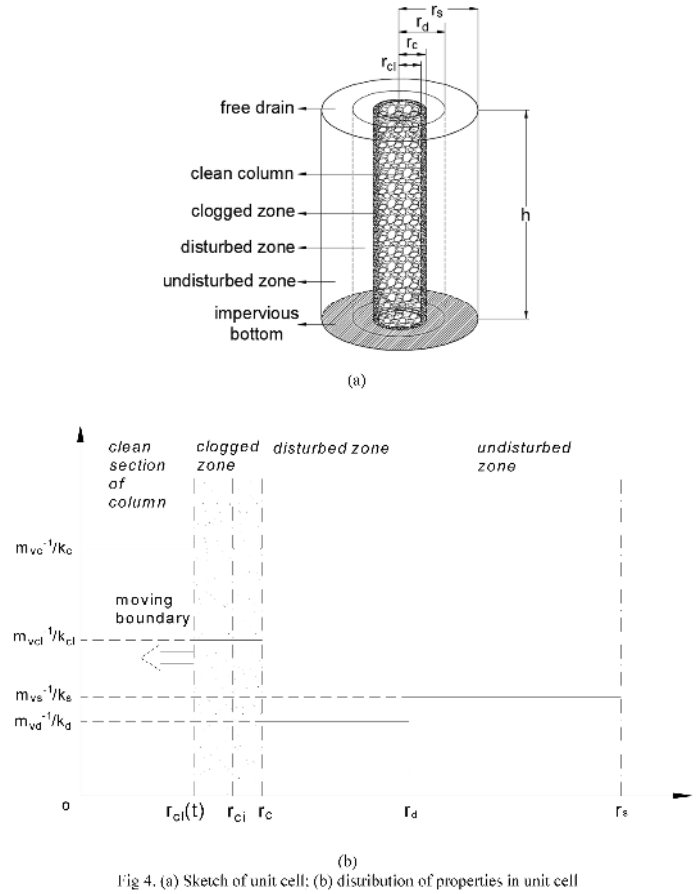

Fig 4. (a) Sketch of unit cell: (b) disiribution of properties in unit cell

Fig 4. (a) Sketch of unit cell; (b) distribution of properties in unit cell

297x420mm (300 x 300 DPI)

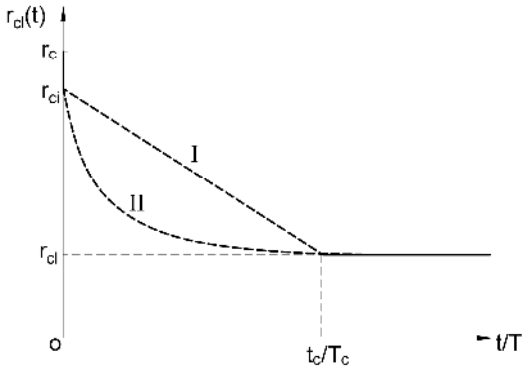

Fig 5. Patterns of clogging development

Fig 5. Patterns of clogging development

297x420mm (300 x 300 DPI)

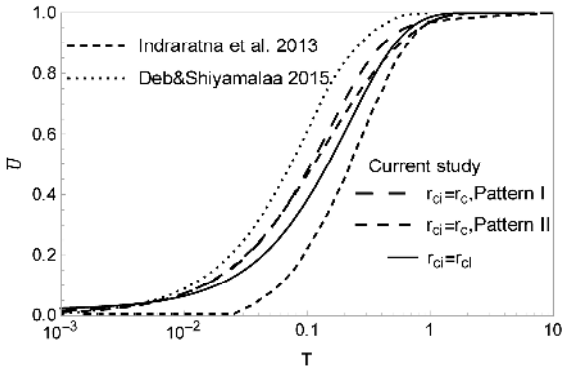

Fig 7. Comparison of consolidation rate with previous studies (including clogging)

Fig 7. Comparison of consolidation rate with previous studies (including clogging)

297x420mm (300 x 300 DPI)

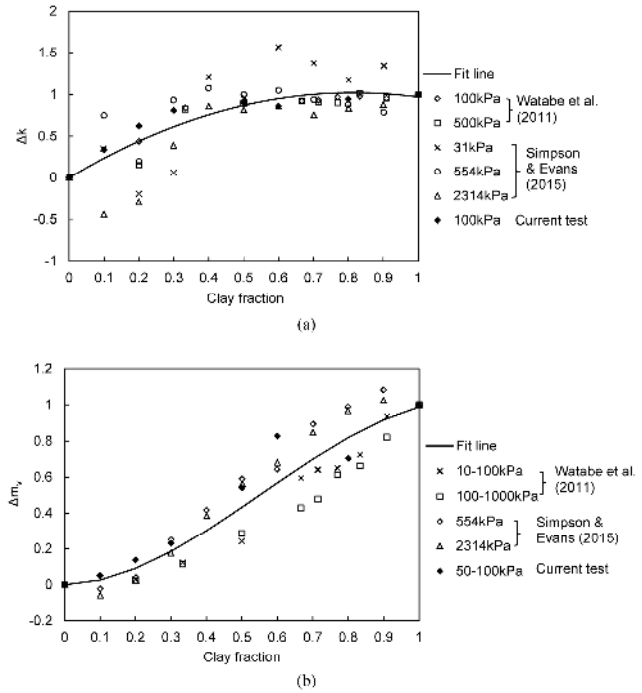

Fig 8. Change of mixture properties with clay fraction: (a) permeability; (b) compressibility

Fig 8. Change of mixture properties with clay fraction: (a) permeability; (b) compressibility

297x420mm (300 x 300 DPI)

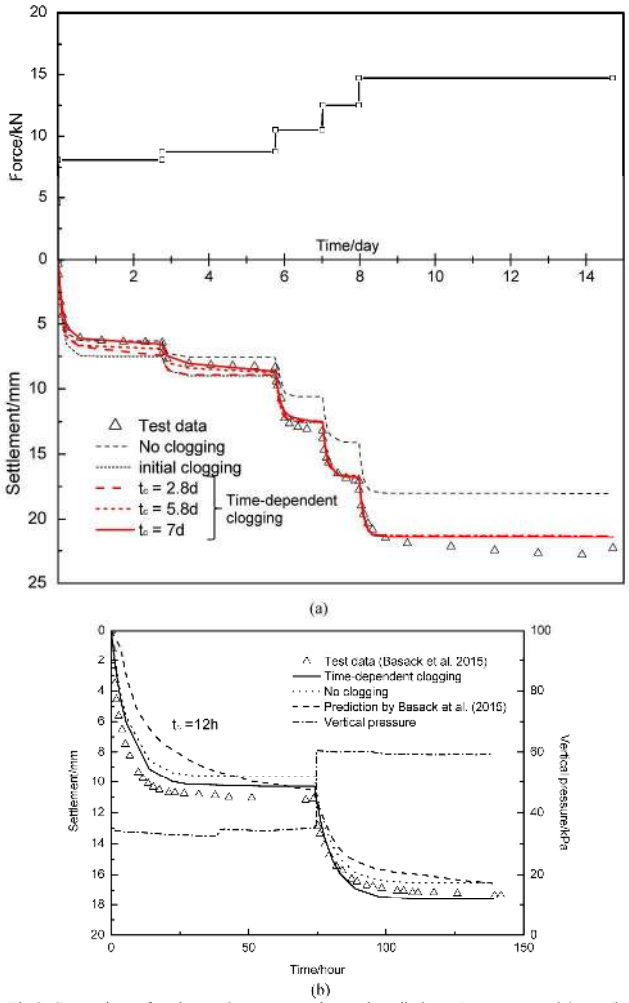

Fig 9. Comparison of settlement between test data and predictions: (a) current model test; (b) model test by Basack et al. (2015)

9

Fig 9. Comparison of settlement between test data and model predictions: (a) current model test; (b) model test by Basack et al. (2015)

297x420mm (300 x 300 DPI)

Appendix

The deduction of equation (10a) is given as below.

Integrating equation (7) regards to radius and using boundary condition (9a) would yield

$$\frac{\partial u_s}{\partial r} = \frac{\gamma_w (r_s^2 - r^2)}{2k_s f(r) r} \frac{\partial \varepsilon_v}{\partial t} \tag{a1}$$

Then substitute (a1) into (8) will obtain:

$$\frac{r_s^2}{r_c^2} \frac{\partial \varepsilon_v}{\partial t} + \frac{\bar{k}_c(t)}{\gamma_w} \frac{\partial^2 u_c}{\partial z^2} = 0 \tag{a2}$$

If combining the integral of equation (a1) with boundary condition (9b), the equations below can be deduced

$$u_s - u_c = \frac{\gamma_w}{2k_s} \frac{\partial \varepsilon_v}{\partial t} \int_{r_c}^{r} \frac{r_s^2 - r^2}{f(r) r} dr \tag{a3}$$

Then the average pore pressure in the surrounding clay can be calculated

$$\bar{u}_s = \frac{1}{\pi (r_s^2 - r_c^2)} \int_{r_c}^{r_s} 2\pi r u_s dr = u_c + \frac{\gamma_w A}{k_s (r_s^2 - r_c^2)} \frac{\partial \varepsilon_v}{\partial t} \tag{a4}$$

Equation (a4) can be manipulated further to obtain a second derivative of u_c regarding to depth.

$$\frac{\partial^2 \bar{u}_s}{\partial z^2} = \frac{\partial^2 u_c}{\partial z^2} + \frac{\gamma_w A}{k_s (r_s^2 - r_c^2)} \frac{\partial^3 \varepsilon_v}{\partial t \partial z^2} \tag{a5}$$

Finally, a unified governing equation (10a) can be obtained by combining (6a), (a2) and (a5).